ARTICLE IN PRESS

Available online at www.sciencedirect.com

SCIENCE DIRECT®

Chemical Physics 300 (2004) 233–238

Chemical Physics

www.elsevier.com/locate/chemphys

Ab initio molecular orbital and RRKM calculations of the thermal decomposition of CH_2BrO radical

Evangelos Drougas, Agnie M. Kosmas *

Physical Chemistry Laboratory, Department of Chemistry, University of Ioannina, 45110 Ioannina, Greece

Received 30 October 2003; accepted 21 January 2004

Abstract

A theoretical study of the thermal decomposition and isomerization channels of bromomethoxy radical is carried out using ab initio molecular orbital methods and RRKM theory. Three kinds of reaction pathways are examined, bond scission, intramolecular three-center HBr elimination and isomerization. Energy-specific rate coefficients $k(E)$ and thermal rate constants $k(T,P)$ are evaluated using the ab initio data and RRKM theory. Relevance to existing experimental evidence is discussed.

1. Introduction

The chemistry of halogenated alkoxy radicals has been a subject of extensive experimental and theoretical investigations as these species are interesting intermediates in the atmospheric oxidation of halogenated hydrocarbons [1–3]. However, most relevant experimental and theoretical studies deal with fluorinated and chlorinated alkoxy radicals [4–12] and less attention has been given to brominated analogs.

The bromomethoxy radical, in particular, is formed in the reaction of CH_3Br with OH, which is the principal loss process for methyl bromide in the atmosphere [13]. Under atmospheric conditions the fate of CH_2BrO radical is expected to be determined either by the reaction with O_2

$$CH_2BrO + O_2 \rightarrow HC(O)Br + HO_2$$

or by unimolecular decomposition through Br-extrusion or HBr elimination

$$CH_2BrO + M \rightarrow CH_2O + Br + M$$

$$CH_2BrO + M \rightarrow HCO + HBr + M$$

Early studies [14,15] suggested that the predominant fate of CH_2BrO radical under atmospheric conditions is reaction with O_2. Later however, the investigation of the degradation process of $BrCH_2O$ formed in the Cl-atom initiated oxidation of CH_3Br, by Chen et al. [16] and Orlando et al. [17], has given very interesting results regarding the fate of bromomethoxy radical. These workers have clearly shown that the unimolecular decomposition of CH_2BrO to $CH_2O + Br$ is the dominant depletion process at 1 atm of O_2 and temperature range 228–298. The reaction with O_2 and the three-center HBr elimination, $CH_2BrO \rightarrow HCO + HBr$, have been found to be minor pathways under these conditions. In view of these experimental findings, the theoretical study of the reactivity of $BrCH_2O$ will also present a lot of interest since no theoretical treatments to the best of our knowledge, exist for the study of dissociation mechanisms of CH_2BrO.

In the present work, a theoretical study of the thermal decomposition and isomerization channels of bromomethoxy radical is carried out using ab initio molecular orbital methods and RRKM theory. The following five reaction channels are considered:

$$CH_2BrO \rightarrow Br + CH_2O \quad (1)$$

$$\rightarrow HBr + CHO \quad (2)$$

$$\rightarrow H + CHBrO \quad (3)$$

$$\rightarrow CBrO + H_2 \quad (4)$$

$$\rightarrow CHBrOH \quad (5)$$

* Corresponding author. Fax: +651-44989.
E-mail address: amylona@cc.uoi.gr (A.M. Kosmas).

0301-0104/$ - see front matter © 2004 Published by Elsevier B.V.
doi:10.1016/j.chemphys.2004.01.021

Reactions (1) and (3) represent the C–Br and C–H bond scission channels while reactions (2) and (4) are three-center elimination channels. Finally, channel (5) is the isomerization pathway to CHBrOH.

The most important stationary points on the potential energy surface are investigated using electronic structure methods. Using these results, energy specific rate coefficients $k(E)$ and thermal rate constants $k(T,P)$ for the most interesting decomposition pathways, channels (1)–(5), are evaluated and the falloff behaviour is examined. The results are discussed in relation with the existing experimental evidence.

2. Computational details

The geometries of reactant, products, and stationary points have been fully optimized at the UMP2(full)/6-31G(d) and UMP2(full)/6-311G(d,p) levels of theory. Harmonic vibrational frequencies have been calculated at the same levels to characterize the stationary points. Transition states were identified by one imaginary frequency as first order saddle points. To refine the energetics G2MP2 [18] calculations were carried out at the UMP2(full)/6-311G(d,p) optimized geometries. The G2MP2 method which is a modified version of G2 [19] using MP2 instead of MP4 for the basis set extension corrections, is considered to reasonably approximate the full G2 method at a substantially reduced computational cost and it is sufficiently suitable for a large system like the present one which involves four heavy atoms. The total G2MP2 energy is given by

$$E_0(\mathrm{G2MP2}) = E[\mathrm{QCISD(T)/6\text{-}311G(d,p)}] + \Delta(\mathrm{MP2}) + \mathrm{HLC} + \mathrm{ZPE}, \quad (6)$$

where

$$\Delta(\mathrm{MP2}) = E[\mathrm{MP2/6\text{-}311+G(3df,2p)}] - E[\mathrm{MP2/6\text{-}311G(d,p)}]. \quad (7)$$

HLC is the higher level correction to account for remaining basis set deficiencies, $\mathrm{HLC} = -\mathrm{Bn}_\alpha - \mathrm{An}_\beta$ (n_α, n_β being the number of α and β electrons, respectively) and ZPE represent the zero-point energy corrections. All calculations have been carried out using the Gaussian 98 series of programs [20].

Two isomeric energy minima and five transition state configurations were investigated for channels (1)–(5) in addition to products. Internal coordinate calculations (IRCs) were performed at the UMP2(full)/6-311G(d,p) level to confirm that each transition state links the reactant and the appropriate products. No symmetry constrains have been imposed in the optimization procedure. The optimized geometries and geometrical parameters for all stationary points examined are shown in Fig. 1. Electronic energies and energy differences are summarized in Table 1 and the relative energy profile for channels (1)–(5) is depicted in Fig. 2. Table 2 lists the harmonic frequencies and the moments of inertia of the two isomeric energy minima and the transition state configurations.

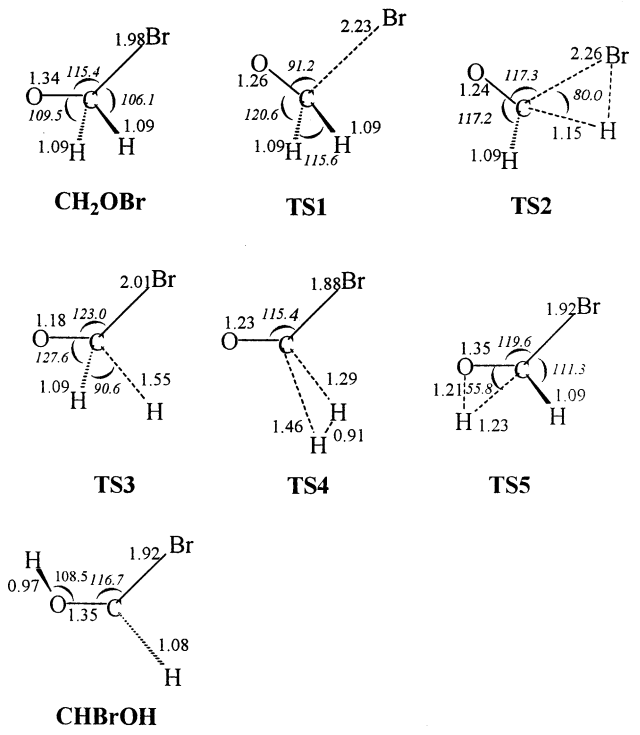

Fig. 1. Optimized structures at the UMP2(full)/6-311G(d,p) level for stationary points of various decomposition and isomerization channels of CH_2BrO.

3. Quantum mechanical results

3.1. Bond scission processes

The ground state CH_2BrO radical presents a similar geometry with the corresponding chlorinated analog and may decompose via C–Br or C–H bond scissions according to channels (1) and (3) through well-defined transition states. Thus, channel (1) leads to the cleavage of the C–Br bond through TS1 to produce $CH_2O + Br$ at 7.2 kcal mol^{-1} below reactant at the G2MP2 level. TS1 results from a simple elongation of the breaking C–Br bond length by 13% and the simultaneous shrinkage of the C–O distance by 6% as a result of the forming carbon–oxygen double bond. The imaginary frequency of 624i cm^{-1} indicates a well-defined transition state geometry and the associated energy barrier is quite low, located only 2.6 kcal mol^{-1} above the reactant at the G2MP2 level. In Fig. 2, this pathway is readily seen to be the most thermodynamically feasible dissociation channel.

Table 1
Total electronic (hartrees) and relative (kcal mol^{-1}) energies and ZPE corrections (kcal mol^{-1}) for CH_2BrO decomposition and isomerization

Species	UMP2/6-311G(d,p)	ΔE^a	G2MP2	ΔE^b	ZPE[c]
CH_2BrO	−2686.666600	0.0	−2686.847974	0.0	16.7
CHBrOH	−2686.688136	−12.5	−2686.863134	−9.5	17.8
TS1	−2686.652087	9.1	−2686.843756	2.6	16.6
TS2	−2686.634745	17.6	−2686.829647	11.5	14.3
TS3	−2686.624229	22.2	−2686.819247	18.0	12.3
TS4	−2686.638255	10.8	−2686.823737	15.2	9.7
TS5	−2686.615328	29.9	−2686.801255	29.3	14.4
$Br + CH_2O$	−2686.687831	−13.0	−2686.859387	−7.2	16.4
CHO + HBr	−2686.727375	−33.0	−2686.862428	−9.1	11.6
CHOBr + H	−2686.655763	1.5	−2686.831424	10.4	11.4
$COBr + H_2$	−2686.689284	−6.7	−2686.867326	−12.1	9.2

[a] Energy differences corresponding to UMP2/6-311G(d,p) including ZPE corrections.
[b] Energy differences corresponding to G2MP2 values.
[c] The zero-point-energy corrections correspond to HF harmonic frequencies scaled by 0.89, as included in the G2MP2 results.

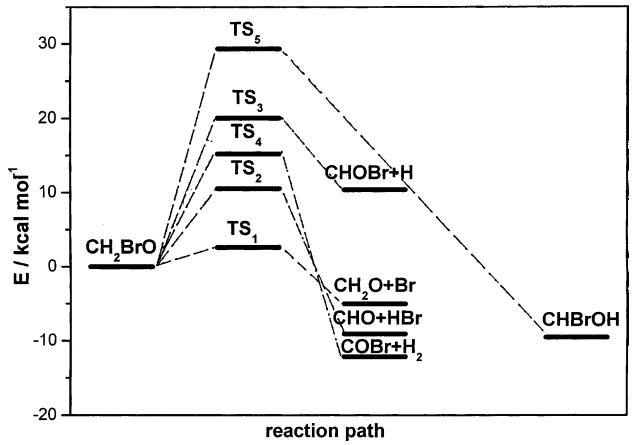

Fig. 2. Energy profile for CH_2BrO unimolecular decomposition and isomerization at the G2MP2 level.

The low barrier height associated with the extrusion of Br atom, 2.6 kcal mol^{-1} at the G2MP2 level, is a quite different feature compared to the analogous barrier values of 11.2 kcal mol^{-1} [6] or 10.5 kcal mol^{-1} [12], calculated at similar levels of theory for Cl-atom extrusion in CH_2ClO decomposition. Similarly opposite patterns have been obtained in the case of α-halogenated ethoxy radicals. In the brominated species [21,22], a very low barrier height for Br-extrusion has been obtained, 1.1 kcal mol^{-1}, in contrast to the higher barrier, 8.2 kcal mol^{-1}, found for C–Cl bond scission in α-chloroethoxy radical [8].

The cleavage of the C–H bond, channel (3), leads to atomic hydrogen and brominated formaldehyde, H + CHBrO, located at 10.4 kcal mol^{-1} above CH_2BrO at the G2MP2 level. These are the only decomposition products less stable than the reactant, due to the breaking of the strong C–H bond. The corresponding transition state TS3 shows larger structural changes than TS1, i.e., a substantial elongation of the breaking C–H bond by 42% and a corresponding shortening of the C–O bond by 12%. The associated energy barrier is higher, 18.0 kcal mol^{-1}, as is readily seen in Fig. 2, making this depletion route rather improbable.

3.2. Elimination processes

Reaction pathways (2) and (4) correspond to three-center eliminations of HBr and H_2, respectively. The HBr elimination takes place through the well-defined transition state configuration TS2 possessing the imaginary frequency at 1964i cm^{-1} and leading to CHO + HBr at 9.1 kcal mol^{-1} below the reactant. TS2 presents a three-membered ring geometry and is formed from the simultaneous stretching of both breaking bonds, the C–H bond increasing to 1.150 Å and the C–Br bond becoming 2.260 Å. The BrCH bond angle also decreases from 106.1° in CH_2BrO to 80.0° inTS2. The

Table 2
Harmonic vibrational frequencies (cm^{-1}) and moments of inertia (amu Å^2) at the UMP2(full)/6-311G(d,p) level of theory

	Harmonic frequencies	I_A, I_B, I_C
CH_2BrO	330, 625, 656, 1064, 1130, 1316, 1429, 3144, 3194	10.6, 131.5, 130.2
CHBrOH	324, 484, 619, 870, 1189, 1300, 1404, 3292, 3857	10.4, 128.5, 137.2
TS1	624i, 242, 776, 1005, 1257, 1415, 1634, 3056, 3094	10.8, 121.1, 132.0
TS2	1964i, 317, 541, 862, 1087, 1359, 1459, 2774, 3056	10.3, 156.5, 163.7
TS3	1801i, 295, 425, 605, 674, 1120, 1315, 1881, 3104	10.6, 134.1, 140.6
TS4	2695i, 312, 339, 365, 620, 1200, 1313, 1373, 2106	14.3, 130.8, 144.4
TS5	2251i, 339, 615, 653, 967, 1242, 1312, 2666, 3212	9.2, 131.6, 139.7

barrier height for HBr elimination is rather high, 11.5 kcal mol^{-1}, significantly higher than the critical energy for Br-atom extrusion. The much higher energy barrier calculated for HBr elimination is again an evidence for the notable differentiation in reactivity between CH_2BrO and the chlorinated analog. In the latter case, the barrier height for HCl elimination has been found to be 8.0 kcal mol^{-1} [12], i.e., lower than the critical energy for Cl-extrusion, 10.5 kcal mol^{-1}, at a similar level of theory. Thus, again similarly opposite trends are observed for hydrogen halide elimination between $ClCH_2O$ and $BrCH_2O$, as in the case of α-chlorinated and α-brominated ethoxy radicals [8,21,22] where also the barrier height for HC1 elimination is lower than the barrier height for HBr elimination. Consequently, Br-extrusion is the most favourable depletion process for the brominated alkoxy radicals whereas HCl loss appears to be the prevailing decomposition channel for the depletion of the chlorinated analogs. We may summarize that the weaker C–Br bond compared to C–Cl leads to certain regularities regarding the fate of haloalkoxy radicals in the atmosphere through dissociation. Carbon–halogen bond scission is a much more efficient depletion process in the case of bromoalkoxy radicals while HCl elimination is the most favourable decomposition channel for the corresponding chlorinated species.

The 1,1 H elimination channel, reaction (4), leads to $H_2 + CBrO$ at 12.1 kcal mol^{-1} below the reactant through TS4. The structure possesses an imaginary frequency at 2695i cm^{-1} and is formed through the considerable elongation of both C–H bonds. As it is seen from Fig. 2, it also exhibits a high barrier, 15.2 kcal mol^{-1}.

3.3. Isomerization process

The only possible rearrangement pathway through TS5 leads to the formation of CHBrOH, more stable than CH_2BrO by 9.5 kcal mol^{-1} at the G2MP2 level. However, the associated isomerization barrier is the highest, 29.3 kcal mol^{-1}, making this channel the least probable reaction pathway. TS5 involves the elongation of the C–H bond by 13% and the decrease of the OCH angle from 109.5° in CH_2BrO to 55.8° in TS5 while the imaginary frequency of 2251i cm^{-1} indicates a well-defined transition state geometry.

4. Reaction kinetics

4.1. Microscopic rate constants

Using the ab initio calculated harmonic frequencies, moments of inertia and barrier heights, we have performed RRKM (Rice–Ramsberger–Kassel–Marcus) calculations [23–25] to determine the rotationally averaged energy-specific microcanonical $k_i(E)$ rate constants for the CH_2BrO unimolecular decomposition and isomerization channels (1)–(5). For simplification purposes, the reverse process of the isomerization reaction (5) that should be included in the accurate treatment of the rate coefficients is omitted in the RRKM calculations considering the much higher energy barrier compared to all other channels. The RRKM algorithm by Zhu and Hase [26] and the UNIMOL package [27] have been used to carry out the kinetic calculations. In particular, energy-specific rate constants for channels (1)–(5) have been computed using both the RRKM algorithm and the first part of the UNIMOL package with results in excellent agreement with each other. Temperature and pressure dependences have been calculated by employing the second part of the UNIMOL algorithm and using suitably adjusted Lennard–Jones parameters for the present brominated radical, calculated in the same way as the corresponding chlorinated analog [12] and taking into account the Br_2 parameters, $\sigma_{Br2} = 4.27$ Å and $\varepsilon_{Br2} = 520$ K [29]. More specifically, the Lennard–Jones collision diameter σ_{AB} was taken equal to 4.48 Å and the Lennard–Jones well depth, ε_{AB} (K), equal to 242 K.

Fig. 3 shows the energy-specific rate constants of channels (1)–(5) as a function of the total energy E. The Br-atom extrusion, channel (1), that possesses the lowest critical energy for reaction presents the largest $k(E)$ at low energies and dominates the decomposition process of CH_2BrO at the low energy region. The other channels follow according to the order of the critical energy values. Thus, below 20 kcal mol^{-1} we have $k_1(E) > k_2(E) > k_4(E) > k_5(E)$. Quickly though, as the energy rises various crossings occur since the relative magnitude of the low frequencies in the transition states begins to play a significant role. Channel (4) which leads to the most thermodynamically stable products, $H_2 + CBrO$, prevails at the high energy range as the low frequencies

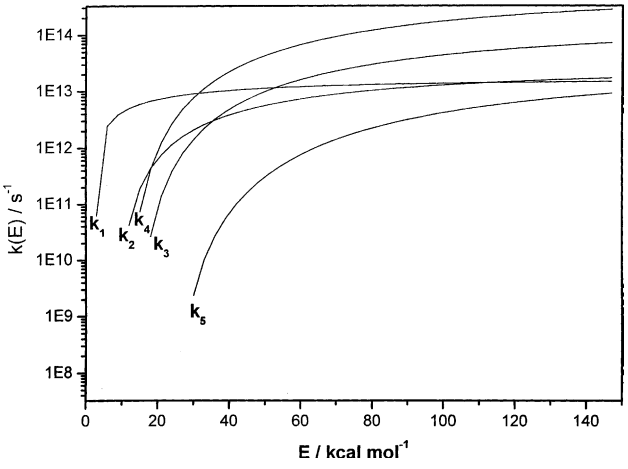

Fig. 3. Energy-specific rate constants $k(E)$ vs E.

of TS4 generally assume the lowest values among all reaction channels. The isomerization channel (5) with the highest critical energy remains lower throughout the entire energy region. In summary, the most important reaction channel for CH_2BrO decomposition is the bond scission C–Br process which is soon surmounted by the H_2 elimination, channel (4) at high energies.

4.2. Thermal rate constants

Quantitative evaluation of the rate coefficients requires the detailed solution to the master equation [28]. Because of the numerical difficulties in such a solution, the unimolecular rate constants could be evaluated reliably only in the narrow but interesting temperature range 200–500 K. First, RRKM calculations were performed for the atmospheric pressure of 760 Torr and N_2 as the bath gas. The calculated Arrhenius expressions $k(T)$ for reactions (1)–(5) in the temperature range 200–500 K are plotted in Fig. 4 and they are given by the following equations:

$$k_1(T) = 4.6 \times 10^9 \exp(-1204/T), \quad (8)$$

$$k_2(T) = 1.3 \times 10^{11} \exp(-5057/T), \quad (9)$$

$$k_3(T) = 4.3 \times 10^{11} \exp(-7741/T), \quad (10)$$

$$k_4(T) = 1.8 \times 10^{11} \exp(-6225/T), \quad (11)$$

$$k_5(T) = 3.0 \times 10^{13} \exp(-14474/T). \quad (12)$$

It is readily seen that Br-extrusion is the dominating decomposition pathway. It is also interesting to note that the theoretically calculated value from the Arrhenius equation (8) for $k_1(T)$, 2.4×10^7 s^{-1}, is in reasonable agreement with the experimental estimate, 3×10^7 s^{-1} at 228 K and 1 atm pressure [17].

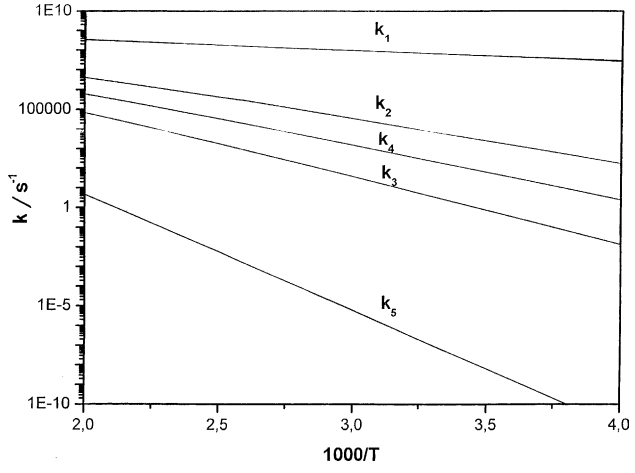

Fig. 4. Thermal rate coefficients for processes (1)–(5) at 1 atm of pressure.

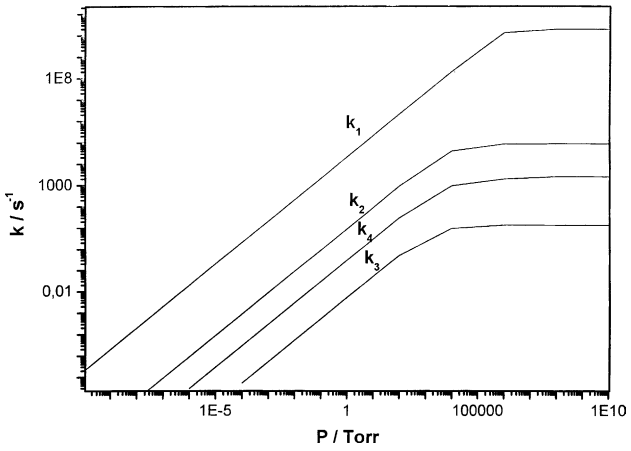

Fig. 5. Falloff plot of the rate constants for reactions (1)–(5) at 298 K with N_2 as the bath gas.

Fig. 5 presents the falloff data for channels (1)–(4) at 298 K. Channel (5) falls out of range. The rate constant of the prevailing C–Br bond scission channel, $k_1(T,P)$, approaches the high-pressure limit near 10^6 Torr. In the neighbourhood of atmospheric pressures within the lower stratospheric region it is readily seen that the rates of all four channels are well within the falloff region.

5. Summary

The most important stationary points on the potential energy surface for the decomposition and isomerization channels of CH_2BrO radical are investigated at the G2MP2 level of theory with the initial optimization of reactants, products, and transition states carried out at the UMP2(full)/6-31G(d) and UMP2(full)/6-311G-(d,p) levels of theory. The energetics has been examined at the G2MP2 methodology. The bromomethoxy radical is less stable than all decomposition and isomerization products with the exception of CHBrO + H products resulting from the C–H bond scission. The most probable unimolecular decomposition pathway is the C–Br bond breaking channel which is consistent with the experimental evidence and contrary to what has been found for the corresponding chlorinated analog where the most probable depletion channel is the three-center HCl elimination.

Energy-specific rate constants $k(E)$ are calculated as a function of total energy using RRKM theory. An evaluation of the thermal rate coefficients $k(T,P)$ is performed using the UNIMOL [27] package for the temperature range 200–500 K. The results indicate that the Br-atom extrusion presents the lowest energy barrier for reaction and thus, it is the most favourable pathway for CH_2BrO decomposition. This is an interesting difference with what happens in the decomposition of the chlorinated analog, CH_2ClO, where the HCl intramo-

lecular elimination is the most important dissociation channel. The same differences are observed with the corresponding ethoxy derivatives, CH_3CHClO and CH_3CHBrO. The calculated prevalence of halogen atom extrusion in the brominated species is also consistent with the experimental evidence which indicates that C–Br bond scission is the most probable depletion channel in CH_2BrO decomposition [16,17].

References

[1] S. Solomon, Nature (London) 347 (1990) 6291.
[2] G.P. Brasseur, J.J. Orlando, Atmospheric Chemistry and Global Change, Oxford University Press, New York, 1999.
[3] R. Zellner, Global Aspects of Atmospheric Chemistry, Steinkopff, Darmstadt, 1999.
[4] V. Catoire, R. Lesclaux, P.D. Lightfoot, M.T. Rayez, J. Phys. Chem. 98 (1994) 2889.
[5] I.E. Mogelberg, J. Shested, T.J. Wallington, O.J. Nielsen, Int. J. Chem. Kin. 29 (1997) 209.
[6] B. Wang, H. Hou, Y. Gu, J. Phys. Chem. A 103 (1999) 2060.
[7] F. Wu, R.W. Carr, Chem. Phys. Lett. 305 (1999) 44.
[8] H. Hou, B. Wang, Y. Gu, J. Phys. Chem. A 104 (2000) 1570.
[9] H. Somnitz, R. Zellner, Physical Chemistry Chemical Physics 3 (2001) 2352.
[10] A. Kukui, G. Le Bras, Physical Chemistry Chemical Physics 3 (2001) 175.
[11] S. Inomata, M. Yamaguchi, N. Washida, J. Chem. Phys. 116 (2002) 6961.
[12] F. Wu, R.W. Carr, J. Phys. Chem. A 106 (2002) 5832.
[13] A. Mellouki, R.K. Talukdar, A.-M. Schmoltner, T. Gierczak, M.J. Mills, S. Salomon, A.R. Ravishankara, Geophys. Res. Lett. 19 (1992) 2059.
[14] O.J. Nielsen, J. Munk, G. Locke, T.J. Wallington, J. Phys. Chem. 95 (1991) 8714.
[15] R. Weller, H. Lorenzen-Schmidt, O. Schrems, Ber. Bunsenges. Phys. Chem. 96 (1992) 409.
[16] J. Chen, V. Catoire, H. Niki, Chem. Phys. Lett. 245 (1995) 519.
[17] J.J. Orlando, G.S. Tyndall, T.J. Wallington, J. Phys. Chem. 100 (1996) 7026.
[18] L.A. Curtiss, K. Raghavachari, J.A. Pople, J. Chem. Phys. 98 (1993) 1293.
[19] L.A. Curtiss, K. Raghavachari, G.W. Trucks, J.A. Pople, J. Chem. Phys. 94 (1991) 7221.
[20] M.J. Frisch et al., GAUSSIAN 98, Gaussian, Inc., Pittsburgh, PA, 1998.
[21] J.J. Orlando, G.S. Tyndall, J. Phys. Chem. A 106 (2002) 312.
[22] E. Drougas, A.M. Kosmas, Chem. Phys. Lett. 379 (2003) 297.
[23] J.I. Steinfeld, J.S. Francisco, W.L. Hase, Chemical Kinetics and Dynamics, Prentice Hall, Englewood Cliffs, NJ, 1989.
[24] T. Baer, W.L. Hase, Unimolecular Reaction Dynamics, Theory and Experiment, Oxford University Press, New York, 1996.
[25] R.G. Gilbert, S.C. Smith, Theory of Unimolecular and Recombination Reactions, Blackwell Scientific Publications, Oxford University Press, 1990.
[26] L. Zhu, W.L. Hase, QCPE 644.
[27] R.G. Gilbert, S.C. Smith, M.J.T. Jordan, UNIMOL Program Suite, Sydney University, NSW, 1993.
[28] J. Troe, J. Chem. Phys. 66 (1977) 4745.
[29] J.O. Hirschfelder, C.F. Curtiss, R.B. Bird, Molecular Theory of Gases and Liquids, Wiley, New York, 1954.